Aromaticity in isoelectronic analogues of benzene, carborazine and borazine: Perspective from electronic structure and magnetic property

Yang Wu, [#a] Xinye Liu, [#a] Xiufen Yan, [a] Zeyu Liu, *[a] Tian Lu, *[b] Jingbo Xu, [a] Jiaojiao Wang [a]

[a]*School of Environmental and Chemical Engineering, Jiangsu University of Science and Technology, Zhenjiang 212100, People's Republic of China*

[b]*Beijing Kein Research Center for Natural Sciences, Beijing 100022, People's Republic of China*

Abstract

Carborazine ($B_2C_2N_2H_6$) and borazine ($B_3N_3H_6$) are isoelectronic analogues of benzene (C_6H_6). The aromatic character of borazine remains a controversial issue, and the related properties of carborazine are even rarely reported. In this work, we systematically investigated the geometric structure, charge distribution, frontier molecular orbital characteristics, magnetic shielding effect, and induced ring current of carborazine and borazine, and compared the studied characteristics with those of benzene to determine the aromatic character of two analogues. The combination of multiple properties shown that although they are isoelectronic, carborazine, like benzene, is strongly aromatic, while borazine only exhibits rather weak aromaticity. The C atom acting as a connecting bridge between B and N atoms reduces the electronegativity difference on the molecular backbone and enhances the electron delocalization over the conjugated path, which is the essence of the distinct disparity of aromaticity between carborazine and borazine.

Keywords: carborazine, borazine, aromaticity, electronegativity, electron delocalization

[#] These authors contributed equally to this work.

* Corresponding authors. E-mail addresses: liuzy@just.edu.cn (Z. Liu), sobereva@sina.com (T. Lu).

1. Introduction

The aromaticity of cyclic molecules is one of the most frequently mentioned properties in modern organic chemistry, and numerous studies have long been conducted on it.[1,2] Aromaticity is not a property that can be observed experimentally, and there is no strict physical definition.[3] Chemists commonly explore molecular aromaticity through a variety of indicators proposed based on different physical ideas or empirical rules. Electron counting rules were first used to assign aromaticity character in π conjugated systems, the most important being Hückel's rule which suggests that planar molecules with $(4n + 2)\pi/4n\pi$ electrons are aromatic/anti-aromatic. Benzene (C_6H_6) is the origin of the word "aromaticity" that conforms perfectly to the Hückel's $(4n + 2)\pi$ electrons rule.

B and N are elements in the periodic table adjacent to C. The substitution of each two C atoms in benzene by a pair of B and N atoms obtains an isoelectronic analogue of benzene. These isoelectronic molecules have the same 6π electrons as benzene, suggesting that, according to the Hückel's rule, they should all be aromatic. However, the fact is not so simple.

As early as 1926, Stock et al.[4] succeeded in experimentally synthesizing an isoelectronic species of benzene, $B_3N_3H_6$, named borazine and popularly known as inorganic benzene, which is formally a product of the complete substitution of the CC unit of benzene by BN, as shown in Scheme 1. Inspired by this synthesis experiment, extensive research has been conducted on the aromaticity of borazine, but the conclusions are inconsistent. For examples, Iwaki and Udagawa[5] investigated the effect of the introduction of heteroatoms into the benzene on the aromaticity through index of deviation from aromaticity (IDA),[6] nucleus-independent chemical shift (NICS),[7] and harmonic oscillator model of aromaticity (HOMA)[8] methods, and the borazine is accordingly proposed to be anti-aromatic, non-aromatic, and aromatic, respectively; Schleyer et al.,[9] after calculating the NICS values separated into the NICS(σ) and NICS(π) contributions, stated that the borazine is not aromatic due to the strong polarity of B-N bond, similar to the conclusion drawn by Jemmis et al.[10] through magnetic

susceptibility exaltation (MSE) and from the NICS analyses; Du and coworkers[11] reported the very small gauge-including magnetically induced current (GIMIC)[12] value for borazine, which indicates that borazine is weakly aromatic; Using the dissected magnetically induced current density (MICD)[13] and aromatic stabilization energy (ASE) in combination with Hückel's as well as Baird rules, Báez-Grez and Pino-Rios[14] also demonstrated that borazine should be considered as a weakly aromatic system, and they argued that the aromaticity is associated with a so-called hidden ring current; Islas et al.[15] split the π molecular orbitals from the σ ones and used the induced magnetic field ($\mathbf{B}^{ind}$) and the electron localization function (ELF) methods to derive that borazine should be described as a π aromatic compound, but it is not globally delocalized; Some energetic-based measures have established the aromaticity of borazine, and the degree is about half of that of benzene.[16] In short, it can be seen that the aromatic character of borazine is still a controversial matter to date.

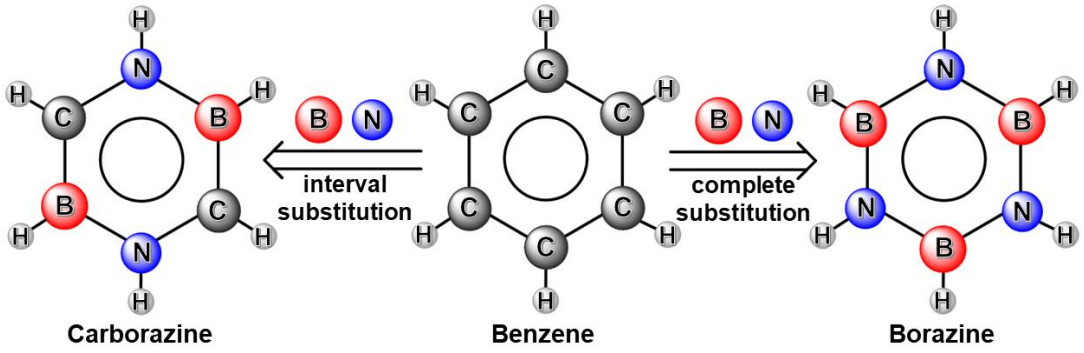

Scheme 1. Structural association of benzene, carborazine, and borazine

In 2015, Srivastava et al.[17] proposed a new isoelectronic analogue of benzene, $B_2C_2N_2H_6$ referred to as carborazine, which is structurally formed by replacing three adjacent C atoms on benzene ring with BCN as the structural fragment, as also shown in Scheme 1. This work pointed out that carborazine has aromatic properties, but in our point of view, the evidence provided is still limited and further investigation is needed.

Nowadays, many aromaticity descriptors have been recommended on the basis of multiple manifestations of molecular aromaticity, including geometrical,[18] energetic,[19]

electronic,[20] and magnetic[21] ones. However, no single metric can be used independently to reliably measure the aromaticity of a particular system, especially for those with unusual electronic structure. So in most cases, one should examine several aromaticity criteria simultaneously and check if the indices reach the same conclusion or correlate well with each other.[22,23] Just recently, a comprehensive theoretical study of the aromaticity of the cyclo[18]carbon (C_{18}) and its isoelectronic species was completed by us.[24,25] The combination of multiple aromaticity metrics suggests that, although $B_6C_6N_6$ and B_9N_9 are both isoelectronic analogues of C_{18}, $B_6C_6N_6$ has a prominent aromaticity comparable to C_{18}, whereas B_9N_9 is a non-aromatic species. Insightful electronic structure analyses indicate that the aromaticity difference between $B_6C_6N_6$ and B_9N_9 arises from the bridging effect of C atoms on the π conjugated path in the former system.

Considering that the aromatic characteristics of carborazine and borazine have not been rigorously revealed, and combined with our recent research experience on the aromaticity of isoelectronic species of C_{18}, here we will make a comprehensive comparative study of the molecular aromaticity of benzene, carborazine, and borazine. The aim of this work is to give a clear answer to the aromaticity characteristics of the isoelectronic analogues of benzene and to clarify the essential reasons for their aromaticity differences.

2. Computational Details

We employed the ωB97XD exchange-correlation functional[26] combined with high quality def2-TZVP basis set[27] to perform structure optimizations to the title molecules. *Ab-initio* molecular dynamics (AIMD) was simulated at relatively cheaper ωB97X-D3[28]/6-311G(d)[29] level. The magnetic property calculations and wavefunction analyses in this paper have also been done at the ωB97XD/def2-TZVP level of theory. The atomization energy (E_a) of benzene, carborazine, and borazine was evaluated as $E_a = \left(xE_B + yE_C + zE_N + 6E_H\right) - E_{B_xC_yN_zH_6}$, where $E_{B_xC_yN_zH_6}$, E_B, E_C, E_N, and E_H are electronic energy of molecular ring (benzene, carborazine, or borazine), B atom, C atom, N atom, and H atom, respectively. The natural population analysis (NPA) was

implemented by NBO 7.0.7,[30] the nucleus-independent chemical shifts (NICS) analysis[7] was completed using the continuous set of gauge transformations (CSGT) method,[31] the anisotropy of the induced current density (ACID) plot was generated via the ACID 2.0 program,[32] the current density map and bond current strength analysis were also determined though the continuous transformation of the origin of the current density (CTOCD-DZ2) method by the SYSMOIC package,[33,34] and the MICD[13] analysis was performed using the GIMIC method.[12] The ACID plots were rendered by POV-ray program and MICD animations were generated with the ParaView program.[35] Molecular orbital (MO), atomic charges except for NPA, Mulliken orbital composition analysis[36], Mayer bond order (MBO), properties at bond critical point (BCP), localized orbital locator (LOL),[34] multi-center bond order (MCBO),[38] and iso-chemical shielding surface (ICSS)[39] were calculated by the Multiwfn 3.8(dev) code.[40]

All density functional theory (DFT) calculations involved in this study were implemented by Gaussian 16 A.03 program,[41] except that AIMD was conducted by ORCA 5.0.4.[42] The molecular structures and isosurface maps were visualized by Visual Molecular Dynamics (VMD) 1.9.3 software.[43]

3. Results and Discussion

3.1 Geometric Structure and Stability of Benzene, Carborazine, and Borazine

The Cartesian coordinates of benzene, carborazine, and borazine are given in Tables S1-S3, respectively. The important structural parameters selected for three isoelectronic species are listed in Table 1. The 1.387 Å of C-C bond lengths in benzene obtained by us is within the range of 1.322-1.416 Å measured by Budzianowski and Katrusiak using X-rays in combination with the pressurized freezing technique[44] and is very close to the value of 1.399 Å measured by Tamagawa et al. using electron diffraction.[45] The experimental B-N bond length of borazine is 1.435 Å,[46] which is similar to our calculated value of 1.426 Å. There are currently no reports on the synthesis of carborazine. The calculated bond lengths of B-C/C-N/N-B of carborazine in the present work are 1.491/1.347/1.434 Å, which are consistent with the results of 1.51/1.37/1.45

Å at the MP2/aug-cc-pVDZ level.[17] The above comparisons of structural parameters indicate that the calculation method for optimizing molecular geometry in this work is applicable. All three isoelectronic analogues are observed to be strictly planar. Benzene displays a D_{6h} point group owing to its congruent C-C and C-H bonds, while carborazine and borazine have C_{2h} and D_{3h} symmetries, respectively, due to the introduction of heteroatoms that reduce the symmetry of the molecules.

Table 1 Point group (PG), ring bond lengths ($R_{i,j}$, in Å), ring bond angles ($a_{i,j,k}$, in °), and atomization energy (E_a, in kcal/mol) of benzene, carborazine, and borazine at the ωB97XD/def2-TZVP level

	PG	$R_{i,j}$		$a_{i,j,k}$		E_a
Benzene	D_{6h}	C-C	1.387	C-C-C	120.0	-1365.7
Carborazine	C_{2h}	B-C	1.491	N-B-C	114.1	-1200.9
		C-N	1.347	B-C-N	119.9	
		N-B	1.434	C-N-B	126.0	
Borazine	D_{3h}	B-N	1.426	N-B-N	117.3	-1225.6
				B-N-B	122.7	

Borazine has already been synthesized and thus known to be stable.[4] To examine whether the purely theoretically designed carborazine is also kinetically stable, 50 ps AIMD simulation was performed for it with step size of 1 fs. For the purpose of comparison, the same simulation study was also conducted on borazine. Given that the simulation time is rather limited due to the expensive computational cost, the simulation is maintained at a very high 1000 K by velocity-rescaling thermostat[47] to accelerate sampling of potential energy surface. The map showing superposition of trajectory snapshots is displayed as Figure 1. It can be seen that neither dissociation nor isomerization occurred for the two isoelectronic species, and the fluctuations caused by molecular thermal vibration of their ring skeletons are limited to a small range. This observation suggests that carborazine has structural stability comparable to borazine,

and therefore synthesis via appropriate routes may be feasible in the future.

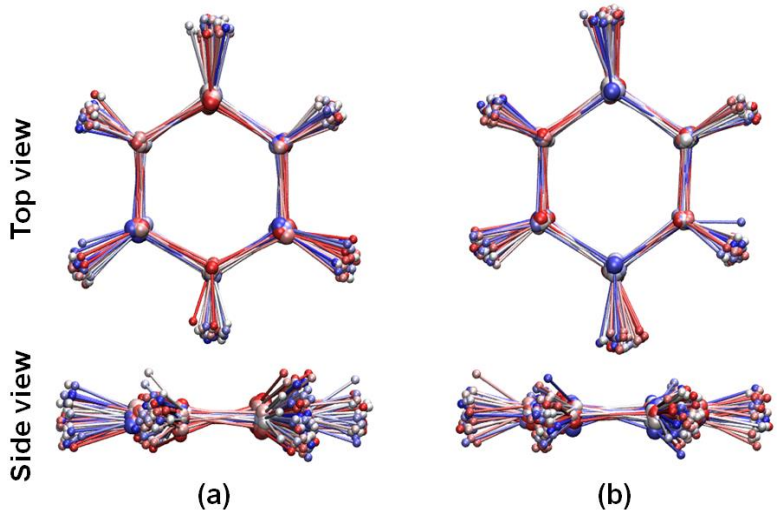

Figure 1. Superposition of trajectory snapshots of (a) carborazine and (b) borazine during 50 ps AIMD simulation. The color varies as blue-white-red according to simulation time. Snapshots are plotted every 1 ps.

The atomization energy (E_a) of molecules is believed to have close relevance to their thermodynamic stability and thus worth to be investigated. We calculated atomization energy of benzene, carborazine, and borazine, and also listed the values in Table 1. It can be seen that the three isoelectronic species all show very large atomic energy, indicating that they are difficult to dissociate to atoms once they are formed. Although E_a of carborazine is notably smaller than that of benzene, it is comparable to that of borazine, which is known to be an experimentally stable molecule. This observation further implies that carborazine should be a synthesizable molecule from thermodynamic point of view.

3.2 Charge Distribution of Benzene, Carborazine, and Borazine

Evaluation of atomic charges is the most straightforward way of quantifying charge distribution in chemical systems[48]. In order to facilitate the understanding of charge distribution in the studied systems, several atomic charge calculation methods,

including natural population analysis (NPA),[49] Hirshfeld method,[50] Hirshfeld-I method,[51] atomic dipole moment corrected Hirshfeld population method (ADCH),[52] and charges from electrostatic potentials using a grid-based method (CHELPG),[53] were applied on benzene, carborazine, and borazine, and the results are shown in Table 2. Despite the significant difference in charge values acquired using different methods for the molecules, the qualitative charge distribution character of the rings is independent of the calculation methods. The distinct difference in electronegativity makes B atoms and N atoms respectively carry evident positive and negative charges in carborazine and borazine. Furthermore, the charge of the C atoms in the carborazine is close to that of the C atoms in benzene, indicating that substitution of two B and two N atoms into benzene does not prominently affect charged state of the remaining C atoms. It can also be seen that the charge difference between B and N atoms in the carborazine is much smaller than that in the borazine, which clearly demonstrates that introducing a C atom between B and N atoms can greatly balance the charge distribution on the ring.

Table 2 Calculated atomic charges (in *e*) of benzene, carborazine, and borazine by different methods

	Atom	NPA	Hirshfeld	Hirshfeld-I	ADCH	CHELPG
Benzene	C	-0.211	-0.043	-0.101	-0.130	-0.085
	H	0.211	0.043	0.101	0.130	0.085
Carborazine	B	0.308	0.013	0.304	-0.090	0.131
	H(B)	-0.047	-0.076	-0.176	-0.033	-0.146
	C	-0.228	-0.053	-0.129	-0.143	-0.125
	H(C)	0.196	0.040	0.102	0.127	0.087
	N	-0.628	-0.064	-0.437	-0.121	-0.230
	H(N)	0.399	0.141	0.337	0.260	0.283
Borazine	B	0.729	0.145	0.973	0.070	0.725
	H(B)	-0.080	-0.070	-0.231	-0.030	-0.213
	N	-1.056	-0.202	-1.138	-0.286	-0.836

H(N)	0.407	0.126	0.396	0.245	0.323

3.3 Frontier Molecular Orbitals of Benzene, Carborazine, and Borazine

The frontier molecular orbital (FMO) characteristics are closely related to the overall electronic delocalization and aromaticity of cyclic molecules. We calculated some FMOs, including all occupied π orbitals, of benzene, carborazine, and borazine, and plotted their energy level maps in Figure 2. Carborazine does not have triple rotation axes like benzene and borazine, which makes it not have double-degenerate highest occupied molecular orbital (HOMO) and lowest unoccupied molecular orbital (LUMO) like the latter two. The HOMO-LUMO gap of carborazine is obviously smaller than that of benzene and borazine, so its chemical stability may be relatively low, and its electrons should show greater softness and are more polarizable.

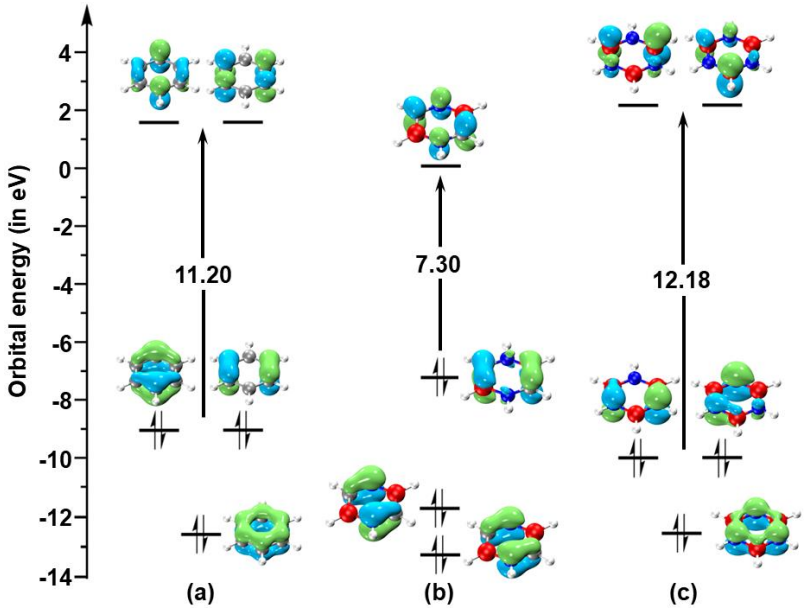

Figure 2. FMO energy level maps (isovalue = 0.07 a.u.) of (a) benzene, (b) carborazine, and (c) borazine. Green and blue colors correspond to the two phases of molecular orbitals. Atom color code: white, H; red, B; grey, C; blue, N.

Among the three isoelectronic species, only the electron delocalization of benzene is uniform. Due to the presence of different elements in rings, the six-center electron

delocalization of carborazine and borazine is definitely weaker than that of benzene. As for which of the latter two has stronger delocalization characteristics, it can be determined by examining the contribution of each element to their occupied π orbitals. The contributions of each element to every occupied π orbital of benzene, carborazine, and borazine calculated by Mulliken method are listed in Table 3. The contribution of the two low-lying orbitals (HOMO-1 and HOMO-2) of carborazine is dominated by N followed by C atoms, while the contribution of B atoms is very small. This is mainly due to the significantly lower energy of the $2p_z$ orbitals of N and C relative to that of B (where z denotes the axis perpendicular to the molecular planes), so they naturally contribute more to the low-lying π orbitals. However, the $2p_z$ orbital of B contributes obviously (more than one third) to the HOMO orbital. Therefore, on the whole, the $2p_z$ orbitals of B, C, and N atoms are all heavily involved in the occupied π orbitals, which inevitably leads to significant six-center conjugation in the carborazine. By comparison, B only participates slightly in the lowest HOMO-1 orbital in borazine, and its participation in the two degenerate HOMO orbitals is even smaller. This observation implies that the global delocalization of π electrons in borazine should be conspicuously more difficult than that in carborazine and benzene.

Table 3 Contributions of each element to every occupied π orbitals in benzene, carborazine, and borazine

	Orbital	B	C	N
Benzene	HOMO	-	99.91%	-
	HOMO	-	99.91%	-
	HOMO-1	-	99.93%	-
Carborazine	HOMO	35.36%	55.29%	9.26%
	HOMO-1	1.72%	17.22%	80.95%
	HOMO-2	8.94%	23.86%	67.10%
Borazine	HOMO	10.41%	-	89.47%
	HOMO	10.41%	-	89.47%

HOMO-1	22.06%	-	77.83%	

3.4 Bonding character of Benzene, Carborazine, and Borazine

We calculated Mayer bond order (MBO),[54] which essentially represents effective number of shared electron pairs between two atoms,[55] to characterize the bonding characters in benzene, carborazine, and borazine. The total MBO and the contributions of σ and π electrons to it are shown in Table 4. From π contribution to MBO, it can be seen that C-C bonds in benzene exhibit more prominent π interactions than those in other molecules, which is in line with the well-known fact that benzene has strong π conjugation. The B-C, C-N, and N-B bonds in carborazine all shows more intensive π interaction than the B-N bond in borazine, indicating that overall π conjugation of carborazine may be stronger than that of borazine. It is worth to note that although the electronegativity of B and N atoms are very different, as shown by the no small π bond order, the sharing of π electrons between the two atoms cannot be underestimated.

Table 4 MBO and various properties at BCP of benzene, borazine, and carborazine[a]

	Bond	MBO			BCP			
		total	σ	π	ρ	$\nabla^2\rho$	H	η
Benzene	C-C	1.406	0.952	0.454	0.321	-0.950	-0.344	2.127
Carborazine	B-C	1.317	0.965	0.352	0.201	0.068	-0.214	0.485
	C-N	1.268	0.874	0.394	0.324	-0.804	-0.520	1.310
	N-B	1.150	0.799	0.351	0.191	0.654	-0.164	0.286
Borazine	B-N	1.199	0.879	0.320	0.204	0.475	-0.193	0.340

[a] Electron density (ρ) and its Laplacian ($\nabla^2\rho$), as well as energy density (H), are in a.u.; eta index (η) is dimensionless.

The LOL based only on π MOs, referred to as LOL-π, is a popular real-space function used to reveal the delocalization of π electrons in conjugated molecular units.[56] The LOL-π isosurfaces of benzene, carborazine, and borazine in Figure 3 depicting the

global delocalization channel of the π electrons in the three molecular rings clearly show the strongest global π electron delocalization of benzene and the pronounced delocalization characteristics of carborazine compared to borazine. The π delocalization in the B-C-N units of carborazine is particularly prominent as shown by the LOL-π isosurface map, while the π conjugation of borazine seems to be hindered on every bond. The LOL-π analysis can be seen as visual evidence for above MBO analysis.

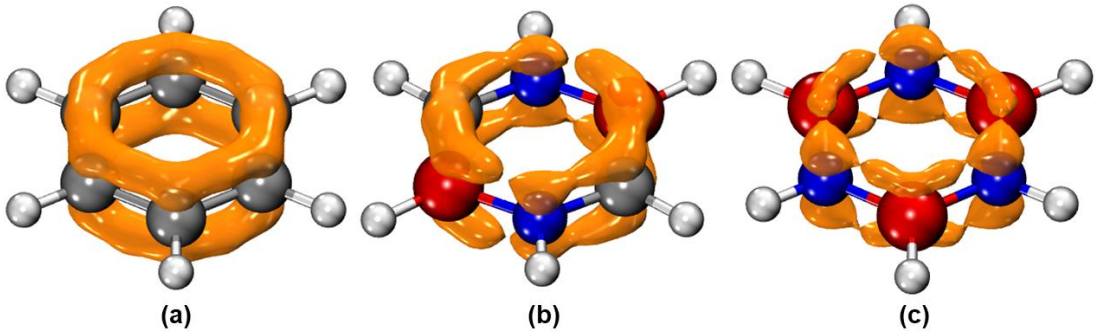

Figure 3. LOL-π isosurfaces (isovalue = 0.5) of (a) benzene, (b) carborazine, and (c) borazine. Atom color code: white, H; red, B; grey, C; blue, N. Atom color code: white, H; red, B; grey, C; blue, N.

The bond critical point (BCP) defined in atoms-in-molecules (AIM) theory is the most representative position of a chemical bond,[57] and its properties are very useful for understanding bonding characteristics. Negative Laplacian of electron density ($\nabla^2\rho$) and energy density (H), as well as eta index (η) larger than 1, usually imply a covalent bond; in addition, the more negative the $\nabla^2\rho$ and H, as well as the larger the η, the stronger the covalency.[58–60] According to the data in Table 4, we find both C-C bond in benzene and C-N bond in carborazine are very typical covalent bond, B-C bond in carborazine has modest covalency, while N-B (also B-N) bond in carborazine and borazine shows most evident ionicity, which obviously is the consequence of the very large difference of electronegativities of the two elements. The data also suggest that the B-N (also N-B) bond in borazine shows stronger σ interaction compared to that in carborazine.

It is noteworthy that in Ref. [15], the authors considered the B-N bonds in borazine to

be essentially ionic as the $\nabla^2\rho$ at the BCP is positive. However, in our opinion, this bond should be referred to as an extremely polar covalent bond because electron sharing character is still prominent on it, as shown by the large value of MBO and negative H at corresponding BCP. The evident localization of electrons around the bond shown by the electron localization function (ELF) map in Figure S1 and the greatly increased electron density during formation of the bond from isolated atoms shown by deformation density (ρ_{def})[61] map in Figure S2 provide supporting evidence for our assertion.

3.5 Magnetic Shielding Effect of Benzene, Carborazine, and Borazine

NICS is a popular method for quantitatively characterizing aromaticity by measuring the shielding effect of an acted external magnetic field at or near center of a ring.[7] It has been confirmed that the normal component of the magnetic shielding tensor at 1 Å above the center of a ring, denoted as NICS(1)$_{zz}$, can robustly reflect its aromatic characteristics.[58] We calculated the total NICS(1)$_{zz}$ values for the three isoelectronic species as well as the contributions of the π electrons and the other electrons (core + σ electrons), respectively, which are listed in Table 5. The total NICS(1)$_{zz}$ of -31.0 ppm for benzene demonstrates its strong aromaticity, which is in accordance with common knowledge of chemistry. The total NICS(1)$_{zz}$ of carborazine is -23.1 ppm, indicating that carborazine is also clearly aromatic, but to a lesser extent than benzene; in contrast, the corresponding value for borazine is -5.21 ppm, a fairly small negative value indicating that it is a weakly aromatic species. The NICS(1)$_{zz}$ values of the isoelectronic analogues studied are in good agreement with those in previous calculations.[17] As is evident from the contributions of the different kinds of electrons to the NICS(1)$_{zz}$, the magnetic shielding at 1 Å above the center of the three isoelectronic rings almost exclusively from their π electrons, while the contribution of the rest of the electrons (core + σ electrons) can be neglected, which suggests that there is no detectable global delocalization of σ electrons in the studied systems, and only π aromaticity is reflected by the NICS(1)$_{zz}$ data.

Table 5 NICS(1)$_{zz}$ (in ppm), ∫NICS$_{zz}$ (in ppm·Å), and MCBO of benzene, carborazine, and borazine[a]

	NICS(1)$_{zz}$			∫NICS$_{zz}$			MCBO
	total	σ+core	π	total	σ	π	
Benzene	-31.0 (-29.52)	-0.94	-30.1	-149.04	-4.52	-146.08	0.0675
Carborazine	-23.1 (-22.48)	0.43	-23.5	-117.95	1.26	-115.80	0.0356
Borazine	-5.21 (-5.19)	0.45	-5.66	-35.95	0.91	-32.58	0.0148

[a] The values obtained from Ref. [17] are given in brackets.

The integrated values of NICS$_{zz}$ curve that vertically crosses a certain ring, denoted as ∫NICS$_{zz}$, is a recently proposed reliable method for quantitatively measuring the aromaticity of cyclic systems.[62,63] A key advantage of ∫NICS$_{zz}$ compared to conventional NICS$_{zz}$ analysis is that it is free from the choice of the point to be studied, thus enabling more rigorous conclusions to be drawn; in the meantime, scanning NICSS$_{zz}$ and its components perpendicular to the ring allows to provide a more comprehensive understanding of molecular aromaticity. As can be seen from the ∫NICS$_{zz}$ listed in Table 5, carborazine has a slightly smaller but still quite obvious negative ∫NICS$_{zz}$ value than benzene, while borazine has a much smaller corresponding value, indicating significant and weak aromaticity of carborazine and borazine, respectively. From Figure 4, it can be seen that the NICS$_{zz}$ curves of the σ electrons of benzene, carborazine, and borazine are almost the same, and the difference in total ∫NICS$_{zz}$ almost entirely comes from the different NICS$_{zz}$ of the π electrons in the three molecules, which is also quantitatively demonstrated by the decomposition of ∫NICS$_{zz}$. It should be noted that the total value (solid lines) of the three isoelectronic species on the NICS$_{zz}$ curve intersects with the component of π electron contribution (dashed lines) near x = 1 Å, meaning that NICS$_{zz}$ at a distance of 1 Å from the ring center is almost exclusively derived from π electrons. The analysis results of ∫NICS$_{zz}$ corroborate the conclusions from the NICS(1)$_{zz}$ calculations above.

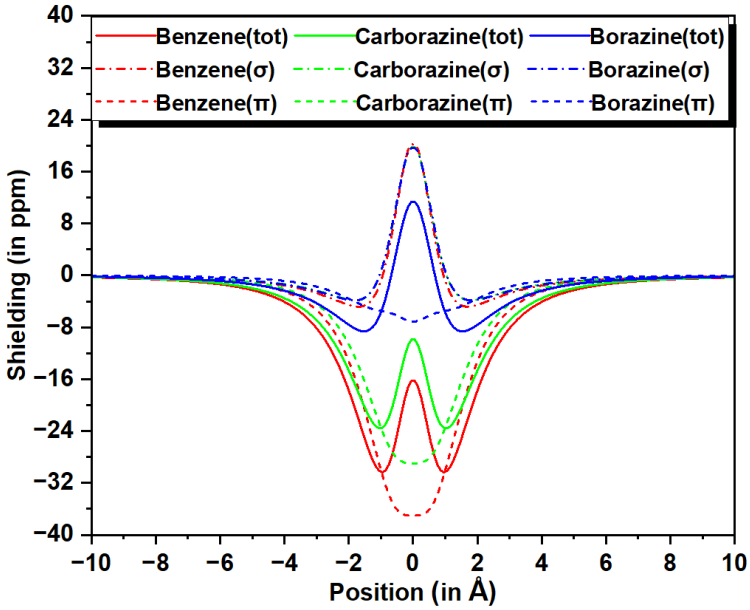

Figure 4. Diagram of NICS$_{zz}$ curves of benzene, carborazine, and borazine.

To verify the conclusions stated from the NICS analyses from electronic structure point of view, we calculated another popular quantitative indicator of molecular aromaticity, the multi-center bond order (MCBO), which is also known as multi-center bond index,[35] and also listed it in Table 5. The comparison reveals that the aromatic characters as reflected by the MCBO value is in line with those obtained through NICS$_{zz}$, namely aromaticity of carborazine is modestly less than benzene but significantly higher than borazine.

The iso-chemical shielding surface (ICSS) analysis visualizes componential magnetic shielding tensor, which is essentially equivalent to extending the NICS analysis to three-dimensional space, providing more comprehensive information about molecular aromaticity.[36] The isosurfaces of *z*-component of the ICSS, referred to as ICSS$_{zz}$,[64] as well as the color-filled contour map of ICSS$_{zz}$ in the slice plane parallel and perpendicular to the plane of benzene, carborazine, and borazine are presented in Figure 5. It can be seen that the ICSS$_{zz}$ isosurfaces of these three molecules are composed of peripheral deshielding region surrounding the central shielding region, and the two regions are concentrated and clear. The consistent ICSS$_{ZZ}$ pattern indicates that both

carborazine and borazine are aromatic like benzene. Upon careful observation, it was found that benzene and carborazine have similar continuous peripheral deshielding isosurfaces at the same isovalue, while the deshielding region of the former is wider, indicating that although carborazine also shows strong aromaticity, its degree is slightly weaker than that of benzene. Prominently, the deshielding isosurfaces of borazine exhibit discontinuity near the H(B) atoms, which intuitively demonstrates that its aromaticity is significantly weaker than that of the carborazine. It is noteworthy that the borazine has a deshielding region wrapped in the shielding isosurface at its ring center, which is apparently due to the insufficient π electron conjugation over the molecular ring. The $NICS_{zz}$ curves in Figure 4 indeed show that over a considerable distance near its center, the $NICS_{zz}$ value of borazine is positive, while the $NICS_{zz}$ of benzene and carborazine are negative at any position. The $NICS_{zz}$ values at the ring centers, referred to as $NICS(0)_{zz}$, are calculated to be of -17.0, -9.61, and 11.9 ppm for benzene, carborazine, and borazine, respectively. Therefore, the $NICS(0)_{zz}$ erroneously determines borazine as an antiaromatic species. From Figure 4, it can be seen that $NICS(0)_{zz}$ is largely contributed by essentially localized σ electrons of the systems, demonstrating that $NICS(1)_{zz}$ is much more reliable than $NICS(0)_{zz}$ in determining π aromaticity.

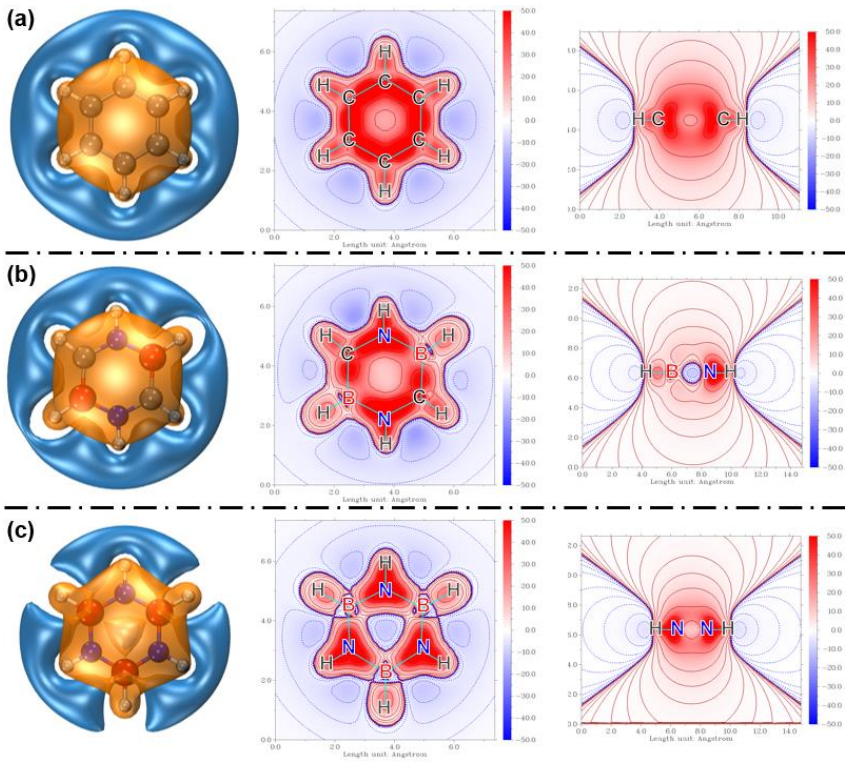

Figure 5. Isosurface maps (left panel, isovalue = 3.0 ppm) and color-filled contour maps (middle and right panels) of (a) benzene, (b) carborazine, and (c) borazine. Orange and blue isosurfaces/contours correspond to shielding and deshielding regions, respectively. The color-filled contour maps are drawn in the slice plane parallel (middle panel) and perpendicular (right panel) to the rings, and the scale of color bars is given in ppm. Atom color code: white, H; red, B; grey, C; blue, N.

3.6 Induced Ring Current of Benzene, Carborazine, and Borazine

The anisotropy of the induced current density (ACID) can visually exhibit the direction and magnitude of the ring currents induced by an applied magnetic field, and has become a popular way to explore molecular aromticity.[32] We separately plotted the ACID maps of π orbitals, σ orbitals, and all molecular orbitals, respectively marked as ACID(π), ACID(σ), and ACID(tot), of benzene, carborazine, and borazine in Figure 6. The homogeneous and continuous ACID(π) isosurfaces and the arrows representing distinct diatropic ring current can be clearly seen for benzene and carborazine, while the ACID(π) isosurfaces of borazine are localized only near the N atom without forming

a global delocalization. The ACID(σ) isosurfaces of the three isoelectronic molecules are essentially the same, exhibiting diatropic ring current surrounding the outer edges of the rings as well as paratropic ring current surrounding the inner edges of the rings. The total ACID(tot) [= ACID(π) + ACID(σ)] obtained by all electrons clearly shows that both benzene and carborazine form a pronounced overall diatropic ring current over the six-membered ring, but the isosurfaces of the latter is slightly narrower. In contrast, on the six-membered ring of borazine, obvious induced currents are mainly formed around each nitrogen atom. This observation again indicates that benzene and carborazine have obvious and comparable aromaticity, while the aromaticity of fully inorganic isoelectronic species, borazine, is extremely weak. The aromaticity difference between them stems from the differences in the global delocalization capability of π electrons, as unveiled earlier.

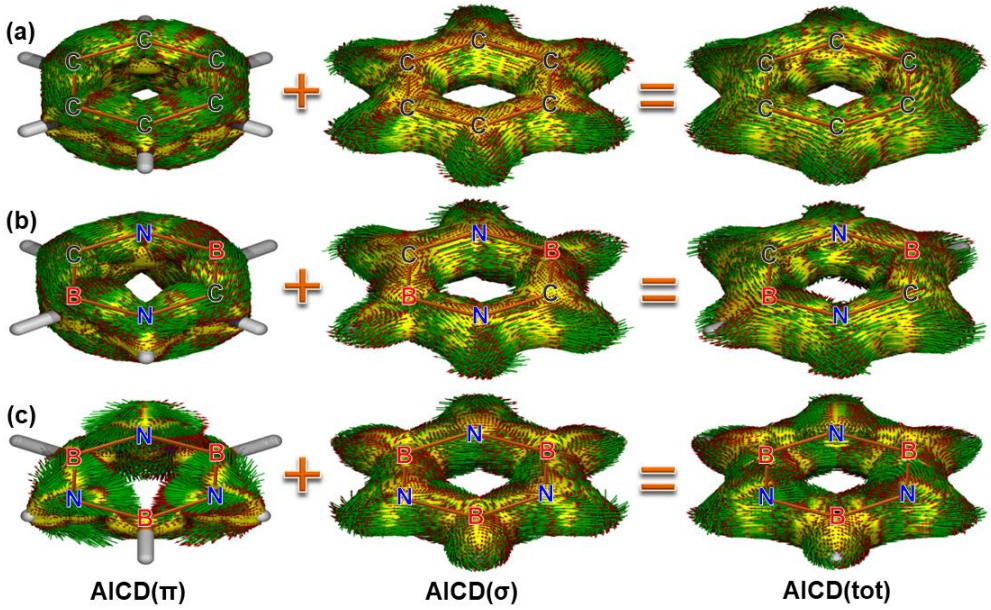

Figure 6. Isosurface maps (isovalue = 0.03 a.u.) of ACID of (a) benzene, (b) carborazine, and (c) borazine.

The CTOCD-DZ2 is an alternative method to reveal the magnetically induced current of chemical systems.[33] We present the current density maps and bond current strengths (BCSs) determined by CTOCD-DZ2 method in Figure 7 for providing a

complementary perspective to the ACID isosurface. The BCS is defined as integral of current density over the plane placed at midpoint of a bond and perpendicular to the bond. As is shown in the top panel, at 1 Bohr above the molecular planes, the diatropic ring current calculated considering all electrons for benzene and carborazine can be readily observed, but the global ring current of borazine is almost invisible in the total current density. The net bond current strengths displayed in the bottom panel can be directly compared with the current density maps drawn in the top panel. The diatropic current strength of C-C bond in benzene is the largest among three isoelectronic species, reaching 12.0 nA/T. The net current strengths of B-C, C-N, and N-B bonds in carborazine are 9.5, 9.8, and 9.6 nA/T, respectively, indicating that the molecule can also form strong currents in an external magnetic field. In contrast, however, the BCS of the B-N bond of borazine is only 3.3 nA/T, which is very small compared to those of its two analogues.

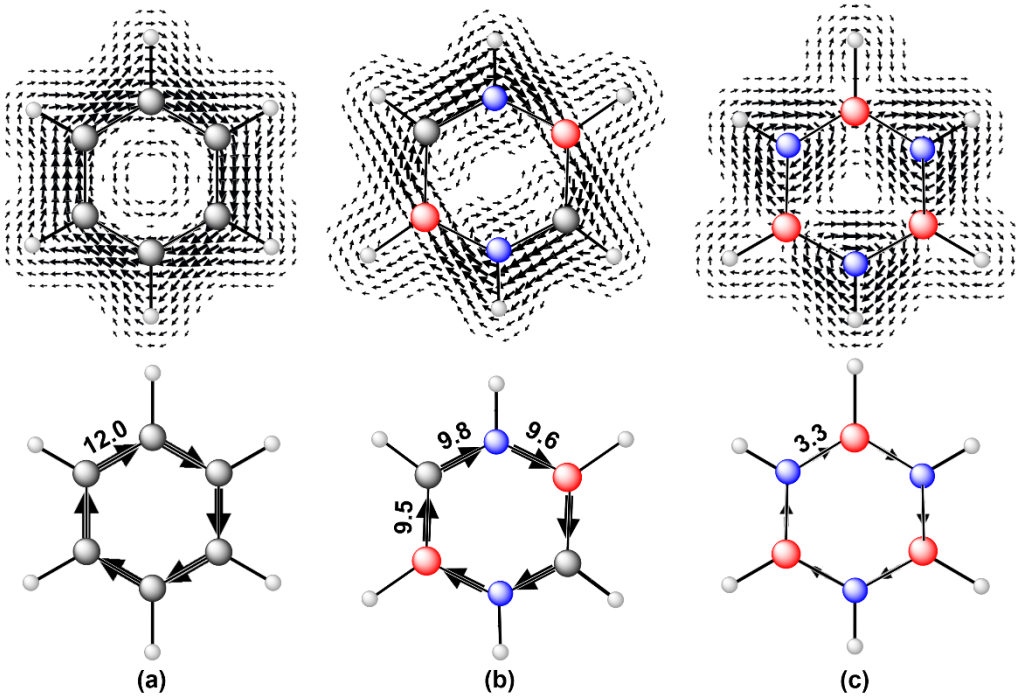

Figure 7. Current density maps over a plane 1 Bohr above the molecular plane (top panel) and bond current strengths (bottom panel) of (a) benzene, (b) carborazine, and (c) borazine. The BCSs are given in nA/T. Atom color code: white, H; red, B; grey, C; blue, N.

Furthermore, we generated animations in the Supporting Information to visually demonstrate the dynamics of the induced ring current for the three isoelectronic analogues using GIMIC method.[12] It can be seen that benzene and carborazine have obvious and similar globally diatropic ring current, while borazine substantially exhibits localized ring currents enveloping around N atoms. Results are in accordance with the above static NICS, MCBO, ICSS, ACID, and CTOCD-DZ2 analyses. Therefore, it confirms once again from a dynamic perspective that the benzene exhibits strongest aromaticity closely followed by carborazine, while the aromaticity of borazine is much lower than theirs. Moreover, the integration of the MICD flowing through a plane intersecting one chemical bond using GIMIC method leads to current strengths of 12.3, 9.4/9.6/9.5, and 3.0 nA/T for benzene, carborazine, and borazine, respectively. These values are in great agreement with the net bond current strengths obtained by the CTOCD-DZ2 method, indicating that the conclusion is independent of the method of evaluating magnetically induced current.

3.7 Role of Bridging C atoms in Carborazine

The essential reasons for the differences in aromaticity of the three isoelectronic species deserve to be explored in depth. In order to investigate the utility of C atom in changing the aromaticity of the isoelectronic analogues of benzene, we analyzed the pre-natural atomic orbitals (PNAOs)[65,66] of atoms of the three molecular rings, as shown in Figure 8. The degree of overlap of the PNAOs is closely related to strength of π interactions. One can see that the order of spatial extent of the $2p_z$ atomic orbitals of the B, C, and N atoms is in the order of B atom > C atom > N atom. In other words, introducing the C atom is equivalent to building a bridge between the B and N atoms that promotes π-electron delocalization, which greatly weakens the serious hinderance to electron conjugation caused by the huge electronegativity difference between the two elements. Similar conclusion has been obtained in the exploration of the aromaticity of isoelectronic species in C_{18}.[24]

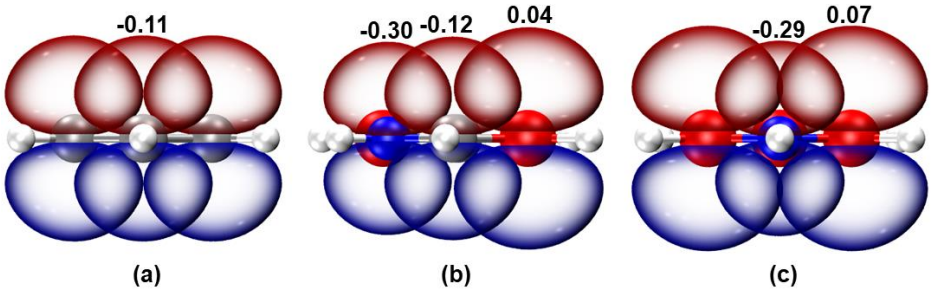

Figure 8. Isosurface maps (isovalue = 0.1 a.u.) of $2p_z$ PNAOs of representative atoms in (a) benzene, (b) carborazine, and (c) borazine. The orbital energies are given in eV. Atom color code: white, H; red, B; grey, C; blue, N.

We also studied several lower symmetry isoelectronic analogues of benzene, named respectively as MOL-1, MOL-2, MOL-3, and MOL-4, for examining the influence of the introduced C atoms on aromaticity of the system. The Cartesian coordinates of these molecular rings are given sequentially in Tables S4-S7. As shown in Figure 9, the first three molecular rings (MOL-1, MOL-2, and MOL-3) exhibit a more negative NICS(1)$_{zz}$ than the MOL-4, and the MOL-2 has the most negative value, even exceeding that of carborazine. The comparison results show that both the number and position of C atoms in the molecular ring affect the aromaticity of the molecule, but the former is much less effective than the latter. So, to summarize, the promotion of aromaticity in B-C-N system mainly depends on the right position of C atoms, that is, they can act as bridges to increase electron global delocalization by balancing electronegativity difference between B and N atoms.

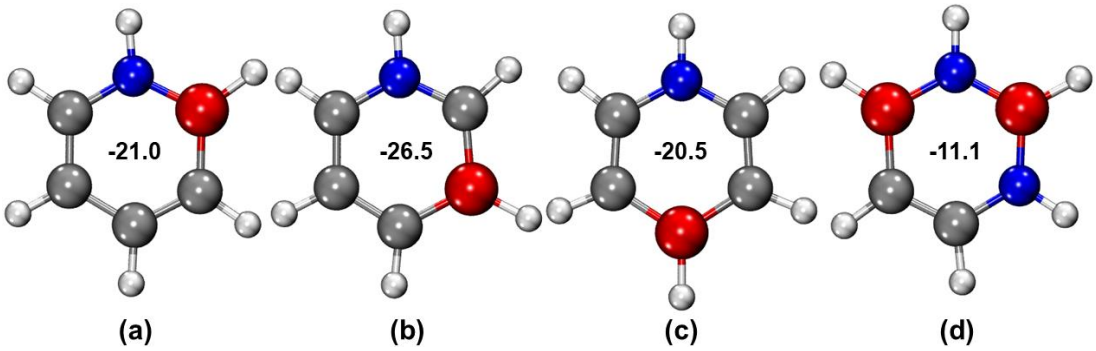

Figure 9. Geometric structures of (a) MOL-1, (b) MOL-2, (c) MOL-3, and (d) MOL-4 optimized at the ωB97XD/def2-TZVP level. The NICS(1)$_{zz}$ values are given in ppm. Atom color code: white, H; red, B; grey, C; blue, N.

4. Conclusions

In this work, the geometric, electronic, bonding, and orbital characteristics, as well as magnetic shielding effect and induced ring current of benzene and its isoelectronic analogues, carborazine and borazine, are theoretically explored, with a focus on in-depth revealing the differences in their aromatic properties. AIMD simulations and E_a analyses first confirmed the thermodynamic stability of the three isoelectronic species. The electronic delocalization of different kinds of chemical bonds was then compared by MBO, properties at BCP, and LOL-π function. Based on the comprehensive analysis of multiple criteria/methods for evaluating aromaticity including NICS, MCBO, ICSS, ACID, CTOCD-DZ2, and MICD, we confirmed that carborazine has definitely aromatic character like benzene, and its aromaticity is only slightly weaker, while borazine is a rather weakly aromatic species. The atomic charge and PNAO analyses revealed the fact that the C atom between B and N in carborazine behaves as an interconnecting bridge that strengthens the electron delocalization over the conjugated path, which is the essence of the significant enhancement of the molecular aromaticity from borazine to carborazine. Moreover, we also examined several six-membered isoelectronic species of the benzene ring with low symmetry, emphasizing the important influence of the location of the introduced C atoms on aromaticity.

The research in this work not only conducts a comprehensive investigation of the electronic structure and aromaticity of various isoelectronic species of benzene, but also highlights the key impact of electron delocalization when C is proper introduced into a system purely composed of B and N. This study will help chemists better understand and design molecules or materials constructed by B, C, and N atoms.

Supporting Information

Optimized Cartesian coordinates of benzene, carborazine, and borazine at the ωB97XD/def2-TZVP level of theory; color-filled map of ELF and contour map of ρ_{def} of borazine; optimized Cartesian coordinates of MOL-1, MOL-2, MOL-3, and MOL-4 at the ωB97XD/def2-TZVP level of theory (PDF)

Notes

The authors declare no competing financial interest.

References

(1) Krygowski, T. M.; Cyrański, M. K. Structural Aspects of Aromaticity. *Chem. Rev.* **2001**, *101* (5), 1385–1420. https://doi.org/10.1021/cr990326u.

(2) Balaban, A. T.; Oniciu, D. C.; Katritzky, A. R. Aromaticity as a Cornerstone of Heterocyclic Chemistry. *Chem. Rev.* **2004**, *104* (5), 2777–2812. https://doi.org/10.1021/cr0306790.

(3) Solà, M. Why Aromaticity Is a Suspicious Concept? Why? *Front. Chem.* **2017**, *5* (22). https://doi.org/10.3389/fchem.2017.00022.

(4) Stock, A.; Pohland, E. Berstoorwassffe, IX.: $B_3N_3H_6$. *Ber. dtsch. Chem. Ges. A/B* **1926**, *59* (9), 2215–2223. https://doi.org/10.1002/cber.19260590907.

(5) Iwaki, R. A.; Udagawa, T. Effect of Heteroatoms on Aromaticity Analyzed by Geometric, Magnetic, and Electronic Criteria. *Chem. Phys. Lett.* **2020**, *745*, 137271. https://doi.org/10.1016/j.cplett.2020.137271.

(6) Sakai, S. New Criterion of Aromaticity and Implications for the (4n + 2)π Rule. *J. Phys. Chem. A* **2003**, *107* (44), 9422–9427. https://doi.org/10.1021/jp030687k.

(7) Chen, Z.; Wannere, C. S.; Corminboeuf, C.; Puchta, R.; Schleyer, P. V. R. Nucleus-Independent Chemical Shifts (NICS) as an Aromaticity Criterion. *Chem. Rev.* **2005**, *105* (10), 3842–3888. https://doi.org/10.1021/cr030088+.

(8) Ostrowski, S.; Dobrowolski, J. Cz. What Does the HOMA Index Really Measure? *RSC Adv.* **2014**, *4* (83), 44158–44161. https://doi.org/10.1039/C4RA06652A.

(9) Schleyer, P. V. R.; Jiao, H.; Hommes, N. J. R. V. E.; Malkin, V. G.; Malkina, O. L. An Evaluation of the Aromaticity of Inorganic Rings: Refined Evidence from Magnetic Properties. *J. Am. Chem. Soc.* **1997**, *119* (51), 12669–12670. https://doi.org/10.1021/ja9719135.

(10) Jemmis, E. D.; Kiran, B. Aromaticity in $X_3Y_3H_6$(X = B, Al, Ga; Y = N, P, As), $X_3Z_3H_3$(Z = O, S, Se), and Phosphazenes. Theoretical Study of the Structures, Energetics, and Magnetic Properties. *Inorg. Chem.* **1998**, *37* (9), 2110–2116. https://doi.org/10.1021/ic970737y.

(11) Du, D.; Sundholm, D.; Fliegl, H. Evaluating Shielding-Based Ring-Current Models by Using the Gauge-Including Magnetically Induced Current Method. *J. Chin. Chem. Soc.* **2016**, *63* (1), 93–100. https://doi.org/10.1002/jccs.201500027.

(12) Fliegl, H.; Taubert, S.; Lehtonen, O.; Sundholm, D. The Gauge Including Magnetically Induced Current Method. *Phys. Chem. Chem. Phys.* **2011**, *13* (46), 20500. https://doi.org/10.1039/c1cp21812c.

(13) Sundholm, D.; Fliegl, H.; Berger, R. J. F. Calculations of Magnetically Induced Current Densities: Theory and Applications. *WIREs. Comput. Mol. Sci.* **2016**, *6* (6), 639–678. https://doi.org/10.1002/wcms.1270.

(14) Báez-Grez, R.; Pino-Rios, R. The Hidden Aromaticity in Borazine. *RSC Adv.* **2022**, *12* (13), 7906–7910. https://doi.org/10.1039/D1RA06457F.

(15) Shen, W.; Li, M.; Li, Y.; Wang, S. Theoretical Study of Borazine and Its Derivatives. *Inorg. Chim. Acta.* **2007**, *360* (2), 619–624. https://doi.org/10.1016/j.ica.2006.08.028.

(16) Timoshkin, A. Y.; Frenking, G. "True" Inorganic Heterocycles: Structures and Stability of Group 13−15 Analogues of Benzene and Their Dimers. *Inorg. Chem.* **2003**, *42* (1), 60–69. https://doi.org/10.1021/ic020361a.

(17) Srivastava, A. K.; Misra, N. Introducing '"Carborazine"' as a Novel Heterocyclic Aromatic Species. *New J. Chem.* **2015**, *39* (4), 2483–2488. https://doi.org/10.1039/C4NJ02089H.

(18) Krygowski, T. M.; Szatylowicz, H.; Stasyuk, O. A.; Dominikowska, J.; Palusiak,

M. Aromaticity from the Viewpoint of Molecular Geometry: Application to Planar Systems. *Chem. Rev.* **2014**, *12* (114), 6383–6422. https://doi.org/10.1021/cr400252h.

(19) Zhu, J.; An, K.; Schleyer, P. V. R. Evaluation of Triplet Aromaticity by the Isomerization Stabilization Energy. *Org. Lett.* **2013**, *15* (10), 2442–2445. https://doi.org/10.1021/ol400908z.

(20) Feixas, F. Quantifying Aromaticity with Electron Delocalisation Measures. *Chem. Soc. Rev.* **2015**, *44* (18), 6434–6451. https://doi.org/10.1039/C5CS00066A.

(21) Gershoni-Poranne, R.; Stanger, A. Magnetic Criteria of Aromaticity. *Chem. Soc. Rev.* **2015**, *44* (18), 6597–6615. https://doi.org/10.1039/C5CS00114E.

(22) Poater, J.; García-Cruz, I.; Illas, F.; Solà, M. Discrepancy between Common Local Aromaticity Measures in a Series of Carbazole Derivatives. *Phys. Chem. Chem. Phys.* **2004**, *6* (2), 314–318. https://doi.org/10.1039/B309965B.

(23) Cyrañski, M. K.; Krygowski, T. M.; Katritzky, A. R.; Schleyer, P. V. R. To What Extent Can Aromaticity Be Defined Uniquely? *J. Org. Chem.* **2002**, *67* (4), 1333–1338. https://doi.org/10.1021/jo016255s.

(24) Wu, Y.; Liu, Z.; Lu, T.; Orozco-Ic, M.; Xu, J.; Yan, X.; Wang, J.; Wang, X. Exploring the Aromaticity Differences of Isoelectronic Species of Cyclo[18]Carbon (C_{18}), $B_6C_6N_6$, and B_9N_9: The Role of Carbon Atoms as Connecting Bridges. *Inorg. Chem.* **2023**, *62* (49), 19986–19996. https://doi.org/10.1021/acs.inorgchem.3c02675.

(25) Liu, Z.; Lu, T.; Chen, Q. An Sp-Hybridized All-Carboatomic Ring, Cyclo[18]Carbon: Bonding Character, Electron Delocalization, and Aromaticity. *Carbon* **2020**, *165*, 468–475. https://doi.org/10.1016/j.carbon.2020.04.099.

(26) Chai, J.-D.; Head-Gordon, M. Long-Range Corrected Hybrid Density Functionals with Damped Atom–Atom Dispersion Corrections. *Phys. Chem. Chem. Phys.* **2008**, *10* (44), 6615–6620. https://doi.org/10.1039/b810189b.

(27) Weigend, F.; Ahlrichs, R. Balanced Basis Sets of Split Valence, Triple Zeta Valence and Quadruple Zeta Valence Quality for H to Rn: Design and Assessment of

Accuracy. *Phys. Chem. Chem. Phys.* **2005**, *7* (18), 3297–3305. https://doi.org/10.1039/B508541A.

(28) Lin, Y.-S.; Li, G.-D.; Mao, S.-P.; Chai, J.-D. Long-Range Corrected Hybrid Density Functionals with Improved Dispersion Corrections. *J. Chem. Theory Comput.* **2013**, *9* (1), 263–272. https://doi.org/10.1021/ct300715s.

(29) Krishnan, R.; Binkley, J. S.; Seeger, R.; Pople, J. A. Self-Consistent Molecular Orbital Methods. XX. A Basis Set for Correlated Wave Functions. *J. Chem. Phys.* **1980**, *72* (1), 650–654. https://doi.org/10.1063/1.438955.

(30) Glendening, E. D.; Landis, C. R.; Weinhold, F. *NBO 6.0* : Natural Bond Orbital Analysis Program. *J. Comput. Chem.* **2013**, *34* (16), 1429–1437. https://doi.org/10.1002/jcc.23266.

(31) Schleyer, P. V. R.; Maerker, C.; Dransfeld, A.; Jiao, H.; Van Eikema Hommes, N. J. R. Nucleus-Independent Chemical Shifts: A Simple and Efficient Aromaticity Probe. *J. Am. Chem. Soc.* **1996**, *118* (26), 6317–6318. https://doi.org/10.1021/ja960582d.

(32) Geuenich, D.; Hess, K.; Köhler, F.; Herges, R. Anisotropy of the Induced Current Density (ACID), a General Method to Quantify and Visualize Electronic Delocalization. *Chem. Rev.* **2005**, *105* (10), 3758–3772. https://doi.org/10.1021/cr0300901.

(33) Zanasi, R. Coupled Hartree–Fock Calculations of Molecular Magnetic Properties Annihilating the Transverse Paramagnetic Current Density. *J. Chem. Phys.* **1996**, *105* (4), 1460–1469. https://doi.org/10.1063/1.472008.

(34) Monaco, G.; Summa, F. F.; Zanasi, R. Program Package for the Calculation of Origin-Independent Electron Current Density and Derived Magnetic Properties in Molecular Systems. *J. Chem. Inf. Model.* **2021**, *61* (1), 270–283. https://doi.org/10.1021/acs.jcim.0c01136.

(35) Ahrens, J.; Geveci, B.; Law, C. ParaView: An End-User Tool for Large-Data Visualization. In *Visualization Handbook*; Elsevier, **2005**; pp 717–731. https://doi.org/10.1016/B978-012387582-2/50038-1.

(36) Lu, T.; Chen, F. Calculation of Molecular Orbital Composition. *Acta Chim. Sinica* **2011**, *69*, 2393–2406. https://doi.org/10.6023/A12030017.

(37) Becke, A. D.; Edgecombe, K. E. A Simple Measure of Electron Localization in Atomic and Molecular Systems. *J. Chem. Phys.* **1990**, *92* (9), 5397–5403. https://doi.org/10.1063/1.458517.

(38) Matito, E. An Electronic Aromaticity Index for Large Rings. *Phys. Chem. Chem. Phys.* **2016**, *18* (17), 11839–11846. https://doi.org/10.1039/C6CP00636A.

(39) Ab Initio Calculation of the Anisotropy Effect of Multiple Bonds and the Ring Current Effect of Arenes—Application in Conformational and Configurational Analysis. *J. Chem. Soc., Perkin Trans. 2* **2001**, No. 10, 1893–1898. https://doi.org/10.1039/b009809o.

(40) Lu, T.; Chen, F. Multiwfn: A Multifunctional Wavefunction Analyzer. *J. Comput. Chem.* **2012**, *33* (5), 580–592. https://doi.org/10.1002/jcc.22885.

(41) Frisch, M. J.; Trucks, G. W.; Schlegel, H. B.; Scuseria, G. E.; Robb, M. A.; Cheeseman, J. R.; Scalmani, G.; Barone, V.; Petersson, G. A.; Nakatsuji, H.; Li, X.; Caricato, M.; Marenich, A. V.; Bloino, J.; Janesko, B. G.; Gomperts, R.; Mennucci, B.; Hratchian, H. P.; Ortiz, J. V.; Izmaylov, A. F.; Sonnenberg, J. L.; Williams; Ding, F.; Lipparini, F.; Egidi, F.; Goings, J.; Peng, B.; Petrone, A.; Henderson, T.; Ranasinghe, D.; Zakrzewski, V. G.; Gao, J.; Rega, N.; Zheng, G.; Liang, W.; Hada, M.; Ehara, M.; Toyota, K.; Fukuda, R.; Hasegawa, J.; Ishida, M.; Nakajima, T.; Honda, Y.; Kitao, O.; Nakai, H.; Vreven, T.; Throssell, K.; Montgomery Jr., J. A.; Peralta, J. E.; Ogliaro, F.; Bearpark, M. J.; Heyd, J. J.; Brothers, E. N.; Kudin, K. N.; Staroverov, V. N.; Keith, T. A.; Kobayashi, R.; Normand, J.; Raghavachari, K.; Rendell, A. P.; Burant, J. C.; Iyengar, S. S.; Tomasi, J.; Cossi, M.; Millam, J. M.; Klene, M.; Adamo, C.; Cammi, R.; Ochterski, J. W.; Martin, R. L.; Morokuma, K.; Farkas, O.; Foresman, J. B.; Fox, D. J. Gaussian 16 Rev. A.03, **2016**.

(42) Neese, F. Software Update: The ORCA Program System, Version 4.0. *WIREs Comput Mol Sci* **2018**, *8* (1), e1327. https://doi.org/10.1002/wcms.1327.

(43) Humphrey, W.; Dalke, A.; Schulten, K. VMD: Visual Molecular Dynamics.

Journal of Molecular Graphics **1996**, *14* (1), 33–38. https://doi.org/10.1016/0263-7855(96)00018-5.

(44) Budzianowski, A.; Katrusiak, A. Pressure-Frozen Benzene I Revisited. *Acta. Crystallogr. B. Struct. Sci.* **2005**, *62* (1), 94–101. https://doi.org/10.1107/S010876810503747X.

(45) Tamagawa, K.; Iijima, T.; Kimura, M. Molecular Structure of Benzene. *J. Mol. Struct.* **1976**, *30* (2), 243–253. https://doi.org/10.1016/0022-2860(76)87003-2.

(46) Chandrasekhar, V.; Nagendran, S. Heteroatomic P-Block (Main-Chain) Polymers. In *Comprehensive Inorganic Chemistry II*; Elsevier, **2013**; pp 823–860. https://doi.org/10.1016/B978-0-08-097774-4.00129-7.

(47) Bussi, G.; Donadio, D.; Parrinello, M. Canonical Sampling through Velocity Rescaling. *J. Chem. Phys.* **2007**, *126* (1), 014101. https://doi.org/10.1063/1.2408420.

(48) Lu, T.; Chen, F. Comparison of Computational Methods for Atomic Charges. *Acta Phys. -Chim. Sin.* **2012**, *28* (01), 1–18. https://doi.org/10.3866/pku.Whxb2012281.

(49) Reed, A. E.; Weinstock, R. B. Natural Population Analysis. *J. Chem. Phys.* **1985**, *83* (2), 735–746. https://doi.org/10.1063/1.449486.

(50) Downward, M. J.; Robb, M. A. The Computation of the Representation Matrices of the Generators of the Unitary Group. *Theoret. Chim. Acta* **1977**, *46* (2), 129–141. https://doi.org/10.1007/BF00548088.

(51) Bultinck, P.; Van Alsenoy, C.; Ayers, P. W.; Carbó-Dorca, R. Critical Analysis and Extension of the Hirshfeld Atoms in Molecules. *J. Chem. Phys.* **2007**, *126* (14), 144111–144119. https://doi.org/10.1063/1.2715563.

(52) Lu, T.; Chen, F. ATOMIC DIPOLE MOMENT CORRECTED HIRSHFELD POPULATION METHOD. *J. Theor. Comput. Chem.* **2012**, *11* (01), 163–183. https://doi.org/10.1142/S0219633612500113.

(53) Breneman, C. M.; Wiberg, K. B. Determining Atom-centered Monopoles from Molecular Electrostatic Potentials. The Need for High Sampling Density in Formamide Conformational Analysis. *J. Comput. Chem* **1990**, *11* (3), 361–373.

https://doi.org/10.1002/jcc.540110311.

(54) Mayer, I. Charge, Bond Order and Valence in the AB Initio SCF Theory. *Chem. Phys. Lett.* **1983**, *97* (3), 270–274. https://doi.org/10.1016/0009-2614(83)80005-0.

(55) Matito, E.; Poater, J.; Solà, M.; Duran, M.; Salvador, P. Comparison of the AIM Delocalization Index and the Mayer and Fuzzy Atom Bond Orders. *J. Phys. Chem. A* **2005**, *109* (43), 9904–9910. https://doi.org/10.1021/jp0538464.

(56) Lu, T.; Chen, Q. A Simple Method of Identifying π Orbitals for Non-Planar Systems and a Protocol of Studying π Electronic Structure. *Theor. Chem. Acc.* **2020**, *139* (2), 25. https://doi.org/10.1007/s00214-019-2541-z.

(57) Bader, R. F. W. *Atoms in Molecules: A Quantum Theory*; Oxford University Press, 1990. https://doi.org/10.1093/oso/9780198551683.001.0001.

(58) Fallah-Bagher-Shaidaei, H.; Wannere, C. S.; Corminboeuf, C.; Puchta, R.; Schleyer, P. V. R. Which NICS Aromaticity Index for Planar π Rings Is Best? *Org. Lett.* **2006**, *8* (5), 863–866. https://doi.org/10.1021/ol0529546.

(59) Niepötter, B.; Herbst-Irmer, R.; Kratzert, D.; Samuel, P. P.; Mondal, K. C.; Roesky, H. W.; Jerabek, P.; Frenking, G.; Stalke, D. Experimental Charge Density Study of a Silylone. *Angew. Chem. Int. Ed.* **2014**, *53* (10), 2766–2770. https://doi.org/10.1002/anie.201308609.

(60) Werner, H.; Paul, W.; Zolk, R. Complexation of PhAs-CH_2 and Synthesis of a Novel $RhAs_3$-Metallaheterocycle. *Angew. Chem. Int. Ed. Engl.* **1984**, *23* (8), 626–627. https://doi.org/10.1002/anie.198406261.

(61) Lu, T.; Chen, Q.; Beijing Kein Research Center for Natural Sciences, Beijing 100022, P. R. China. Revealing Molecular Electronic Structure *via* Analysis of Valence Electron Density. *Acta Phys.-Chim. Sin.* **2018**, *34* (5), 503–513. https://doi.org/10.3866/PKU.WHXB201709252.

(62) Stanger, A. Reexamination of NICSπ,Zz: Height Dependence, Off-Center Values, and Integration. *J. Phys. Chem. A* **2019**, *123* (17), 3922–3927. https://doi.org/10.1021/acs.jpca.9b02083.

(63) Dudek, W. M.; Ostrowski, S.; Dobrowolski, J. Cz. On Aromaticity of the Aromatic

α-Amino Acids and Tuning of the NICS Indices to Find the Aromaticity Order. *J. Phys. Chem. A* **2022**, *126* (22), 3433–3444. https://doi.org/10.1021/acs.jpca.2c00346.

(64) Liu, Z.; Lu, T.; Hua, S.; Yu, Y. Aromaticity of Hückel and Möbius Topologies Involved in Conformation Conversion of Macrocyclic [32]Octaphyrin(1.0.1.0.1.0.1.0): Refined Evidences from Multiple Visual Criteria. *J. Phys. Chem. C.* **2019**, *123* (30), 18593–18599. https://doi.org/10.1021/acs.jpcc.9b06302.

(65) Glendening, E. D.; Landis, C. R.; Weinhold, F. Natural Bond Orbital Methods. *WIREs. Comput. Mol. Sci.* **2012**, *2* (1), 1–42. https://doi.org/10.1002/wcms.51.

(66) Badenhoop, J. K.; Weinhold, F. Natural Bond Orbital Analysis of Steric Interactions. *J. Phys. Chem. C.* **1997**, *107* (14), 5406–5421. https://doi.org/10.1063/1.474248.

Table of Contents:

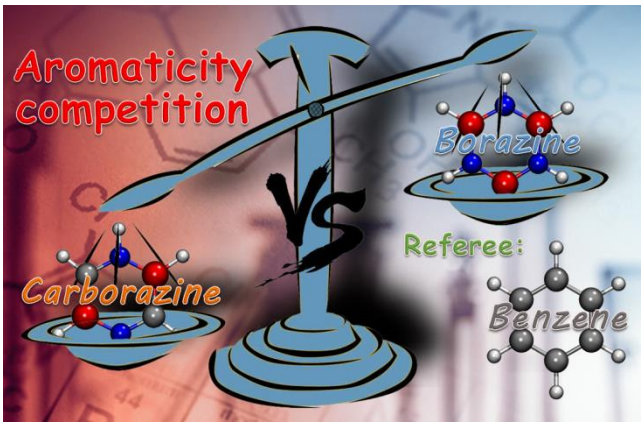

Synopsis:

The geometric, electronic, bonding, and orbital characteristics, as well as magnetic shielding effect and induced ring current of carborazine and borazine were theoretically studied and compared with those of benzene. The combination of multiple properties shown that carborazine, like benzene, is strongly aromatic, while borazine only exhibits rather weak aromaticity. The C atom between B and N atoms in carborazine behaves as an interconnecting bridge that strengthens the electron delocalization over the conjugated path, which is the essence of the distinctly different aromaticity between the isoelectronic analogues of benzene.